Science in China Series D: Earth Sciences

www.scichina.com
earth.scichina.com
www.springerlink.com

The spatial scaling effect of continuous canopy Leaves Area Index retrieved by remote sensing

XU XiRu, FAN WenJie† & TAO Xin

Institute of Remote Sensing and GIS, Peking University, Beijing 100871, China

Leave Area Index (*LAI*) is one of the most basic parameters to describe the geometric structure of plant canopies. It is also important input data for climatic model and interaction model between Earth surface and atmosphere, and some other things. The spatial scaling of retrieved *LAI* has been widely studied in recent years. Based on the new canopy reflectance model, the mechanism of the scaling effect of continuous canopy Leaf Area Index is studied, and the scaling transform formula among different scales is found. Both the numerical simulation and the field validation show that the scale transform formula is reliable.

spatial scaling effect, remotely sensed *LAI*, the true *LAI*, the reflectance model of continuous canopy

Leave Area Index (*LAI*) is one of the most basic parameters to describe the geometric structure of plant canopies. It is also an important input parameter for climatic model and interaction model between earth surface and atmosphere, and some other things[1−7]. Accurate *LAI* retrieval is one basic task of remote sensing application. The spatial scaling of retrieved *LAI* has gained full attention in recent years. Many studies show that if the resolution of remote sensing image is different, the retrieved *LAI* values are also different. Generally speaking, the retrieved *LAI* values from coarse resolution image are lower than the values from fine resolution image, which depends on the nonlinearity of inversion method and the spatial heterogeneity[2,8−16]. MODIS *LAI* products were evaluated by multi-scaling validation, and results show that the inversion error is larger than usual when a kind of vegetation mixed with other kinds of vegetation along with scale increasing[12,13]. The inhomogeneous distribution of vegetation can result in scaling effect. According to these thesis, "spatial scaling" means the resolution of sensor, and spatial scaling effect means the difference between the *LAI* values retrieved from images with different resolution. When discussing the scaling effect of remotely sensed *LAI*, the following basic questions should be answered: What are the basic reasons for the existence of spatial scaling effect? Does the relationship exist between scaled *LAI* with different resolutions? How do we find the transfer formulation of it?

The inversion problem of *LAI* depends on a number of factors. First of all, the reflectance model is the fundamental issue, and the reflectance of canopy is different when the geometry of sun-target-sensor changes, so the difference of retrieved *LAI* caused by this should not be confused with scaling effect. Secondly, the information of plant and soil must be included in the measured signal simultaneously, but the soil reflectance depends on the soil type, the water content, and so on. Therefore, soil background information should be removed from measured signal before discussing spatial scaling effect of *LAI*. Of course, the atmospheric effect should also be excluded. Many researchers discuss the scaling effect based on the empirical relationships between values of

Received September 13, 2007; accepted March 17, 2008
doi: 10.1007/s11430-009-0024-0
†Corresponding author (email: fanwj@pku.edu.cn)
Supported by National Basic Research Program of China (Grant No. 2007CB714402) and National Natural Science Foundation of China (Grant Nos. 40401036, 40734025 and 40401036)

LAI and vegetation indices, such as *NDVI* and *RVI*. But the limitations of such methods are well known, because the problems mentioned above could not be solved satisfactorily, the scaler diagram between *LAI* and vegetation index is not consentaneous, and the degree of dispersion is large, so the new model for retrieval of *LAI* should be found before discussing the spatial scaling effect.

1 The concept and definition of *LAI*

LAI is defined as one half of the total green leaf areas per unit horizontal ground surface area[17], but the boundary of horizontal ground surface area and the spatial distribution of vegetation have not yet been clarified in definition[18]. Suppose a pixel (its area is A) consists of two components: the vegetation and soil (heterogeneity), the vegetation is homogeneously distributed in a_1, the area a_2 is occupied by soil only, the boundary of two areas can approximately be the vertical projection area of leaves, and the area of the pixel $A=a_1+a_2$ (Figure 1).

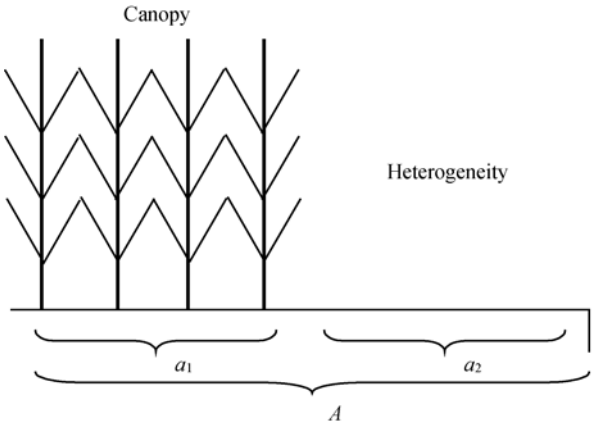

Figure 1 The composition of mixed pixel.

According to the traditional definition of *LAI*, two expressions can be given for *LAI* of the mixed pixel:

$$LAI_{\mathrm{t}} = \frac{LA}{a_1}, \tag{1}$$

$$LAI_{\mathrm{a}} = \frac{LA}{A}, \tag{2}$$

where LA is one half of the total leaves area in unit horizontal ground surface area. It is obvious that the physical meaning of the two definitions is different: LAI_{t} can indicate the real growing condition of plant canopy and accords with definition of crop sowing area, so it is called true *LAI* in this paper. LAI_{a} is *LAI* of the mixed pixel, so it is called apparent *LAI*. The difference between the two definitions is that heterogeneous patch is excluded from the first definition, and the homogenous distribution of vegetation is supposed to be in a_1, but the apparent *LAI* is on the opposite side. Its value is always smaller than true *LAI*, because the same leaves area is divided by larger area. Does the true *LAI* exist in real remote sensing image? The area mainly distributed by continuous canopies is measured by multi-scale sensors, and the area ratio (a_{v}) of vegetation in the pixels is statistically analyzed. The SPOT-5 multi-spectrum image of May 6, 2005 of Jining City, Shandong Province was chosen as the study area. The winter wheat field was in the mature stage with typically continuous canopy character. The results are shown in Figure 2. The horizontal axis means value of a_{v}, and value ranges from 0 to 1. $a_{\mathrm{v}}=1$ means pure vegetation pixel, $a_{\mathrm{v}}=0$ means heterogeneity pixel. The vertical axis represents the characteristics of probability density distribution of a_{v}. The lines represent different resolutions of image, which means the resolution is 20 m × 20 m, 50 m × 50 m, and so on.

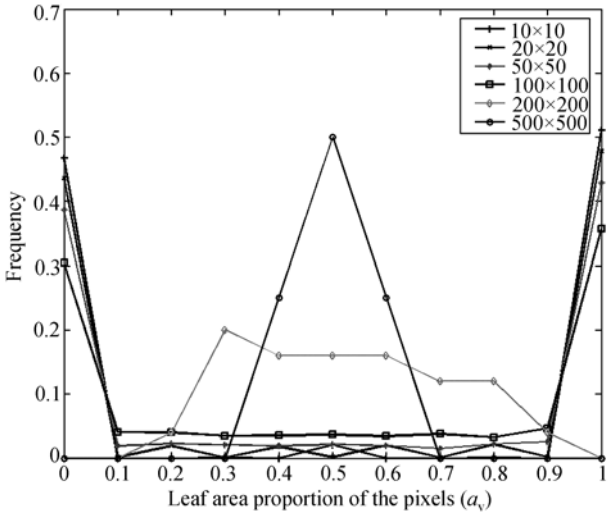

Figure 2 The probability density distribution of a_{v} in images with different resolutions.

Figure 2 shows that along with decreasing of the pixel scale, the ratio of pure pixels increases, and ratio of mixed pixel reduces. The probability density of a_{v} is high for the two extreme values of a_{v}, and low for the intermediate values. When the size of pixel increases, the probability density of the extreme value of $a_{\mathrm{v}+}$ decreases, the probability density is high for the intermediate value of a_{v}, and low for the extreme value of a_{v}.

Here most of pixels are mixed pixel, and the pure pixel almost disappears. By this token, for the continuous canopy, along with the decreasing of the scale, a scale that is macroscopically fine but microcosmically coarse can be found. In this scale, the ratio of mixed pixels can be neglected, and the spatial distribution of leaves within pixel is approximately homogenous, therefore, the *LAI* measured on this scale can be regarded as true *LAI*, and we call it zero-order scale. Any remote sensing image with scale lager than zero-order can be regarded as the mosaic of zero-order scale image. As the true *LAI* of zero-order scale varies in spatial, the true *LAI* of the mixed pixel should be the area ratio weighted summation of true *LAI* of zero-order pixels. The scaling correction of *LAI* actually means deriving the true *LAI* value from the apparent *LAI* retrieved from the remote sensing image.

2 The basic formula for *LAI* scaling effect study

The research target is continuous canopy; the height of canopy is H. There are four components within the field of view of sensor, which are illuminated as ground and canopy, as well as shadowed ground and canopy; K_g, K_c, K_z and K_t represent area ratios of the four parts. Reflectance of targets can be described by $\rho=\rho^1+\rho^m$, here ρ^1 means the single scattering reflectance and ρ^m means the reflectance caused by multiple scattering[19−22]:

$$K_g = e^{-\lambda_0\left[\frac{G_s}{\mu_0}+\frac{G_v}{\mu_v}-\frac{G_v}{\mu_v}\cdot\Gamma(\phi)\right]LAI}, \tag{3}$$

$$K_z = e^{-\lambda_0\frac{G_v}{\mu_v}\cdot LAI} - e^{-\lambda_0\left[\frac{G_S}{\mu_0}+\frac{G_v}{\mu_v}-\frac{G_v}{\mu_v}\cdot\Gamma(\phi)\right]LAI}, \tag{4}$$

$$K_c = 1 - e^{-\lambda_0\frac{G_v}{\mu_v}\cdot LAI\cdot\Gamma(\phi)}, \tag{5}$$

$$K_t = \left(1 - e^{-\lambda_0\frac{G_v}{\mu_v}\cdot LAI}\right) - \left(1 - e^{-\lambda_0\frac{G_v}{\mu_v}\cdot LAI\cdot\Gamma(\phi)}\right) = e^{-\lambda_0\frac{G_v}{\mu_v}\cdot LAI\cdot\Gamma(\phi)} - e^{-\lambda_0\frac{G_v}{\mu_v}\cdot LAI}, \tag{6}$$

where G_v and G_s mean G function of view direction and sun direction; $\mu_v=\cos\theta_v$ and $\mu_0=\cos\theta_0$, where θ_v and θ_0 are the viewing zenith angle and the sun zenith angle respectively. Nilson parameter (λ_0) is used to describe the clumping effect of foliage[23]. $\Gamma(\phi)$ is an empirical function used to describe hot spot effect. ϕ is the angle between light and viewing directions. $\Gamma(0)=1$, $\Gamma(\pi)=0$, $0<\phi\leqslant\pi$, and $\Gamma(\phi)=1-\phi/\pi$.

Radiance of single scattering received by the sensor is L^1, $L^1=K_gL_g+K_zL_z+K_cL_c+K_tL_t$. L_g, L_c, L_z and L_t represent radiance of illuminated ground and canopy, as well as shadowed ground and canopy respectively; f_g and f_v stand for BRDF of ground and canopy respectively. $L_g=f_g(\mu_0F_0+E_d)$, $L_z=f_gE_d$, $L_c=f_v(\mu_0F_0+E_d)$, $L_t=f_vE_d$, and suppose $\rho^1=\pi L^1/(\mu_0F_0+E_d)$, μ_0F_0 is the direct irradiance of sun, and E_d is the diffuse irradiance of atmosphere; suppose leaf and soil are the entire diffuse reflective surface, ρ_g and ρ_v are the hemispherical albedos of the soil background and the leaf, then

$$\rho^1 = \rho_g\left\{e^{-\lambda_0\left[\frac{G_S}{\mu_0}+\frac{G_v}{\mu_v}-\frac{G_v}{\mu_v}\cdot\Gamma(\phi)\right]LAI} + \left[e^{-\lambda_0\frac{G_v}{\mu_v}\cdot LAI} - e^{-\lambda_0\left[\frac{G_S}{\mu_0}+\frac{G_v}{\mu_v}-\frac{G_v}{\mu_v}\cdot\Gamma(\phi)\right]LAI}\right]\frac{E_d}{\mu_0F_0+E_d}\right\} + \rho_v\left\{\left(1-e^{-\lambda_0\frac{G_v}{\mu_v}\cdot LAI\cdot\Gamma(\phi)}\right) + \left[e^{-\lambda_0\frac{G_v}{\mu_v}\cdot LAI\cdot\Gamma(\phi)} - e^{-\lambda_0\frac{G_v}{\mu_v}\cdot LAI}\right]\frac{E_d}{\mu_0F_0+E_d}\right\}. \tag{7}$$

Eq. (7) includes the reflective anisotropic characteristic caused by sun-target-sensor geometry, neglecting the reflective anisotropic characteristic caused by the soil background and the leaf. As $\phi=0$ (hotspot location), then

$$\rho^1 = \rho_g e^{-\lambda_0\frac{G_v}{\mu_v}\cdot LAI} + \rho_v\left(1-e^{-\lambda_0\frac{G_v}{\mu_v}\cdot LAI}\right).$$

If $b=\lambda_0\frac{G_v}{\mu_v}$, then

$$\rho^1 = \rho_g e^{-b\cdot LAI} + \rho_v(1-e^{-b\cdot LAI}). \tag{8}$$

The contribution of multi-scattering can be expressed by Hapke model[24,25]:

$$\rho^m = \frac{\omega}{4}\cdot\frac{1}{\mu_v\mu_0}\left[H(\mu_v)H(\mu_0)-1\right]I_{ms}, \tag{9}$$

where ω is single scattering albedo of single leaf, $\omega\cong 2\rho_v$,

$$H(\mu_{0,v}) = \frac{1+2\mu_{0,v}}{1+2\mu_{0,v}\sqrt{1-\omega}},$$

$$I_{\mathrm{ms}}=\frac{1}{\Delta'}(1-\mathrm{e}^{-\Delta'\cdot\lambda_0\cdot LAI}),\qquad \Delta'=\frac{G_{\mathrm{s}}}{\mu_0}+\frac{G_{\mathrm{v}}}{\mu_{\mathrm{v}}}.$$

When ϕ=0, $\rho^{\mathrm{m}}=\rho_{\mathrm{v}}\dfrac{\left[H^2(\mu_{\mathrm{v}})-1\right]}{4\mu_{\mathrm{v}}G_{\mathrm{v}}}(1-\mathrm{e}^{-2b\cdot LAI})$.

If $m=\dfrac{\left[H^2(\mu_{\mathrm{v}})-1\right]}{4\mu_{\mathrm{v}}G_{\mathrm{v}}}$ and $\rho^{\mathrm{m}}=m\cdot\rho_{\mathrm{v}}\left(1-\mathrm{e}^{-2b\cdot LAI}\right)$,

then

$$\rho=\rho^{1}+\rho^{\mathrm{m}}\cong\rho_g\mathrm{e}^{-b\cdot LAI}+\rho_{\mathrm{v}}(1+m)(1-\mathrm{e}^{-b\cdot LAI}).$$

Since the leaves of the canopy can form gaps by shading each other and the gap can weaken the multiple scattering, the approximate expression can counteract the effect of overestimation caused by Hapke model. As the multiscattering effect is considered, ρ_{v} should be equivalently modified. Suppose $\rho'_{\mathrm{v}}=\rho_{\mathrm{v}}(1+m)$, we have

$$\rho\cong\rho_g\mathrm{e}^{-b\cdot LAI}+\rho'_{\mathrm{v}}(1-\mathrm{e}^{-b\cdot LAI}).\qquad(10)$$

The forms of formulae (10) and (8) are coherent. When $\phi\neq0$, if ρ_g, ρ_{v} and b are modified, the form of formula (8) can be kept. So formula (8) can become the basic formula for *LAI* scaling effect study. During the deduction of formulae (10) and (8), some approximation and parameters are introduced, hereby, the retrieval of *LAI* can not absolutely avoid the influence of factors, such as BRDF, and the variation of soil background. Yet as the formula keeps the fundamental characteristic of canopy reflectance, it can be adapted to different soil backgrounds by adjusting ρ_{g} and correct the errors due to the geometry, clumping effect, LAD, and so on, when b is adjusted. In conclusion, compared with precise *LAI* retrieving model, the precision of formula (10) is a little lower. But it can be feasible to discuss the scaling effect caused by *LAI* spatial variation, and is easy to inverse.

3 The physical mechanism of scaling effect

Supposing pixel A is composed of two small pixels called sub-pixel 1 and sub-pixel 2, the *LAI* of them is LAI_1 and LAI_2 respectively, where $LAI_2=LAI_1+\Delta LAI$. The average *LAI* of pixel A, namely, the apparent *LAI*, is $LAI_{\mathrm{a}}=(LAI_1+LAI_2)/2=LAI_1+\Delta LAI/2$, and the range of ΔLAI is $-LAI_1\to\infty$. As $\Delta LAI=-LAI_1$, and $LAI_2=0$, the sub-pixel 2 is heterogeneous, and according to the definition of the true *LAI*, $LAI_{\mathrm{t}}=LAI_1$, but $LAI_{\mathrm{a}}=LAI_1/2$; except this condition, $LAI_2>0$, and $LAI_{\mathrm{a}}=LAI_{\mathrm{t}}$. In conclusion, $LAI_{\mathrm{a}}\leqslant LAI_{\mathrm{t}}$.

Scenario 1 To keep the spatial inhomogeneity of sub-pixel, $\Delta LAI\neq0$, the multi-scattering between two sub-pixels is neglected, and the reflectance of mixed pixel, $\rho_{\mathrm{A,m}}$, should be the summation of the reflectance of sub-pixel (ρ_1 and ρ_2) weighted by the area ratio:

$$\begin{aligned}\rho_{\mathrm{A,m}}&=\frac{1}{2}(\rho_1+\rho_2)\\&=\frac{1}{2}(\rho_{\mathrm{g}}-\rho_{\mathrm{v}})\mathrm{e}^{-b\cdot LAI_1}\left(1+\mathrm{e}^{-b\cdot\Delta LAI}\right)+\rho_{\mathrm{v}}.\end{aligned}$$

If the *LAI* of pixel A $LAI_{\mathrm{A,m}}$ is retrieved by formula (10), then

$$\begin{aligned}b\cdot LAI_{\mathrm{A,m}}&=-\ln\left[\frac{\rho_{\mathrm{A,m}}-\rho_{\mathrm{v}}}{\rho_{\mathrm{g}}-\rho_{\mathrm{v}}}\right]\\&=-\ln\left[\frac{1}{2}\mathrm{e}^{-b\cdot LAI_1}\left(1+\mathrm{e}^{-b\cdot\Delta LAI}\right)\right].\end{aligned}\qquad(11)$$

Scenario 2 The spatial inhomogeneity of sub-pixel is neglected, the *LAI* of pixel A is average *LAI*, $LAI_1+\Delta LAI/2$, and the relationship between the reflectance of mixed pixel, $\rho_{\mathrm{A,s}}$, and the average *LAI*, $LAI_{\mathrm{A,a}}$, is shown as follows:

$$\begin{aligned}\rho_{\mathrm{A,s}}&=(\rho_{\mathrm{g}}-\rho_{\mathrm{v}})\mathrm{e}^{-b\cdot LAI_1}\mathrm{e}^{-\frac{1}{2}b\cdot\Delta LAI}+\rho_{\mathrm{v}}\\&=\frac{1}{2}(\rho_{\mathrm{g}}-\rho_{\mathrm{v}})\mathrm{e}^{-b\cdot LAI_1}\cdot2\mathrm{e}^{-\frac{1}{2}b\cdot\Delta LAI}+\rho_{\mathrm{v}},\\b\cdot LAI_{\mathrm{A,a}}&=-\ln\left[\frac{\rho_{\mathrm{A,s}}-\rho_{\mathrm{v}}}{\rho_{\mathrm{g}}-\rho_{\mathrm{v}}}\right]\\&=-\ln\left[\frac{1}{2}\mathrm{e}^{-b\cdot LAI_1}\cdot2\cdot\mathrm{e}^{-\frac{1}{2}b\cdot\Delta LAI}\right],\end{aligned}\qquad(12)$$

$$\mathrm{e}^{-b\cdot LAI_{\mathrm{A,m}}}-\mathrm{e}^{-b\cdot LAI_{\mathrm{A,a}}}=\frac{1}{2}\mathrm{e}^{-b\cdot LAI_1}\left(1-\mathrm{e}^{-\frac{1}{2}b\cdot\Delta LAI}\right)^2\geqslant0.\qquad(13)$$

If $\Delta LAI\neq0$, $LAI_{\mathrm{A,m}}<LAI_{\mathrm{A,a}}\leqslant LAI_{\mathrm{t}}$.

The difference between the two scenarios is: the spatial variation of *LAI* is kept in Scenario1, but it is neglected by the average *LAI* for Scenario 2. So if the spatial variation of *LAI* exists within the pixel, the retrieved *LAI* of the pixel is definitely smaller than the true *LAI*. LAI_{t} and LAI_{a} of two scenarios are the same, but the

retrieved *LAI* is different, which is the scaling effect of *LAI*. Two conclusions can be gained as follows:

(1) The inhomogeneity ($\Delta LAI \neq 0$) and non-linear algorithms are the necessary and sufficient preconditions for the existence of spatial scaling effect. $\Delta LAI \neq 0$ is due to two reasons: 1) the variation of *LAI* within pixel exists, 2) the pixel is the heterogeneously mixed pixel; the two reasons are equally important. In other words, the inhomogeneity of *LAI* is the reason for the existence of *LAI* scaling effect. In fact, the retrieval model is based on homogeneous condition; if the formula is forced to the opposite condition, errors would be inevitable.

(2) The spatial scaling effect can only reduce the value of *LAI* smaller than true *LAI* value. Pixel A covers the spatial variation of *LAI* within Pixel A; as pixel size rises, the scale of spatial variation of *LAI* covered by pixel also increases. Each rank reduces retrieved value of *LAI* in certain level. So the apparent *LAI* (LAI_{a}) decreases correspondingly as the pixel size increases, which accords with the fact.

4 The scale transform model

4.1 The description of scale

The spatial scale of remote sensing image is the spatial resolution of pixel *r*. In this paper, the concept of relative scale r_{R} and scale order are put forward:

$$r_{\mathrm{R}} = \frac{r}{r_0}, \tag{14}$$

where r_0 is zero-order scale of pixel. In this scale, almost no mixed pixels exist, and vegetation homogenously distributes in the pixel. If the ratio of two adjacent orders' scales is a constant d, then

$$r_{\mathrm{R}} = d^n \ (\text{or} \quad n = \log_d r_{\mathrm{R}}). \tag{15}$$

So n=0 means r=r_0, and the retrieved *LAI* is true *LAI*, represented by LAI_0; if $n \geqslant 1$, the value of *LAI* is LAI_n, and the scaling effect of *LAI* exists. The scale transform of *LAI* is just the relationship between LAI_n and LAI_0.

4.2 The scaling transform formula neglecting the spatial variation of *LAI*

For zero-order pixels, we have

$$\rho_0 = \left(\rho_{\mathrm{g}} - \rho_{\mathrm{v}}\right)\mathrm{e}^{-b\cdot LAI_0} + \rho_{\mathrm{v}}. \tag{16}$$

Supposing there are N pixels of zero-order in the first-order pixel, and $LAI_{0,i}$ represents the true *LAI* of number i zero-order pixel, $LAI_{0,i} = LAI_{0,\mathrm{a}} + \Delta LAI_{0,i}$. Here $LAI_{0,\mathrm{a}}$ is the mean true *LAI* value of all zero-order pixels in the first-order pixel:

$$\frac{1}{N}\sum_{i=1}^{N} LAI_{0,i} = LAI_{0,\mathrm{a}} + \frac{1}{N}\sum_{i=1}^{N}\Delta LAI_{0,i}$$

and then

$$\begin{aligned}\rho_{0,\mathrm{a}} &= \frac{1}{N}\sum_{i=1}^{N}\rho_{0,i} \\ &= \left(\rho_{\mathrm{g}} - \rho_{\mathrm{v}}\right)\mathrm{e}^{-b\cdot LAI_{0,\mathrm{a}}}\cdot\frac{1}{N}\sum_{i=1}^{n}\mathrm{e}^{-b\cdot\Delta LAI_{0,i}} + \rho_{\mathrm{v}}.\end{aligned}$$

Supposing $\Delta LAI_{0,i} = 0$,

$$\rho_{0,\mathrm{a}} = \left(\rho_{\mathrm{g}} - \rho_{\mathrm{v}}\right)\mathrm{e}^{-b\cdot LAI_{0,\mathrm{a}}} + \rho_{\mathrm{v}}. \tag{17}$$

Assuming m_1 represents the area ratio of zero-order pixels totally occupied by heterogeneity within first-order pixel, the area ratio of vegetative zero-order pixels within first-order pixel is $a_{\mathrm{v},1}$ ($m_1 = 1 - a_{\mathrm{v},1}$), then

$$\begin{aligned}\rho_1 &= (1-m_1)\rho_{0,\mathrm{a}} + m_1\rho_{\mathrm{g}} \\ &= (\rho_{\mathrm{g}} - \rho_{\mathrm{v}})\mathrm{e}^{-b\cdot LAI_{0,\mathrm{a}}} + \rho_{\mathrm{v}} + m_1[(\rho_{\mathrm{g}} - \rho_{\mathrm{v}})(1 - \mathrm{e}^{-b\cdot LAI_{0,\mathrm{a}}})], \\ \rho_1 - \rho_{\mathrm{v}} &= (\rho_{\mathrm{g}} - \rho_{\mathrm{v}})[1 - a_{\mathrm{v},1}(1 - \mathrm{e}^{-b\cdot LAI_{0,\mathrm{a}}})].\end{aligned} \tag{18}$$

If the mixed pixel of first-order can be regarded as an integer, the next formula is tenable:

$$\begin{aligned}\rho_1 &= (\rho_{\mathrm{g}} - \rho_{\mathrm{v}})\mathrm{e}^{-b\cdot LAI_1} + \rho_{\mathrm{v}}, \\ b\cdot LAI_1 &= -\ln\left(\frac{\rho_1 - \rho_{\mathrm{v}}}{\rho_{\mathrm{g}} - \rho_{\mathrm{v}}}\right) = -\ln[1 - a_{\mathrm{v},1}(1 - \mathrm{e}^{-b\cdot LAI_{0,\mathrm{a}}})].\end{aligned} \tag{19}$$

This formula indicates the function between the LAI_1 of the first-order pixel and the mean value of true *LAI* of zero-order pixel $LAI_{0,\mathrm{a}}$.

Similarly, the area ratio of the first-order pixels totally occupied by heterogeneity within the second-order pixel is represented by m_2, and the area ratio of vegetative first-order pixels within the second-order pixel is represented by $a_{\mathrm{v},2}$ (m_2=1–$a_{\mathrm{v},2}$), so

$$\begin{aligned}\rho_2 &= (1-m_2)\rho_{1,\mathrm{a}} + m_2\rho_{\mathrm{g}}, \\ \rho_{1,\mathrm{a}} &= \frac{1}{N}\sum_{i=1}^{N}\rho_{1,i},\end{aligned} \tag{20}$$

where $\rho_{1,i}$ represents the spatial variation of ρ_1 caused by the spatial variation of m_1, which can be expressed by $m_{1,i}$; hereby the average space of $\rho_{0,\mathrm{a}}$ is extended from the first order to the second one, and if the assumed

condition does not change, then

$$\rho_2 = (1-m_2)\left[\left(\rho_g - \rho_{0,a}\right)m_{1,a} + \rho_{0,a}\right] + m_2\rho_g, \quad (21)$$

where $\left(\rho_g - \rho_{0,a}\right) = \left(\rho_g - \rho_v\right)\left(1 - e^{-b\cdot LAI_{0,a}}\right)$,

$$\begin{aligned}&\left(\rho_g - \rho_{0,a}\right)m_{1,a} + \rho_{0,a}\\ &= \left(\rho_g - \rho_v\right)m_{1,a}\left(1 - e^{-b\cdot LAI_{0,a}}\right) + \left(\rho_g - \rho_v\right)e^{-b\cdot LAI_{0,a}} + \rho_v\\ &= \rho_g - \left(\rho_g - \rho_v\right)a_{v,1,a}\left(1 - e^{-b\cdot LAI_{0,a}}\right).\end{aligned}$$

Substituting the above into formula (21), we have

$$\begin{aligned}\rho_2 &= a_{v,2}\rho_g - \left(\rho_g - \rho_v\right)a_{v,2}a_{v,1,a}\left(1 - e^{-b\cdot LAI_{0,a}}\right)\\ &\quad + \rho_g - a_{v,2}\rho_g\\ &= \left(\rho_g - \rho_v\right)\left[1 - a_{v,2}a_{v,1,a}\left(1 - e^{-b\cdot LAI_{0,a}}\right)\right] + \rho_v,\end{aligned}$$

where $a_{v,2} = 1 - m_2$, and if the mixed pixel of second order can be regarded as an integer, the next formula is tenable:

$$\rho_2 = \left(\rho_g - \rho_v\right)e^{-b\cdot LAI_2} + \rho_v,$$

$$\begin{aligned}b\cdot LAI_2 &= -\ln\left(\frac{\rho_2 - \rho_v}{\rho_g - \rho_v}\right)\\ &= -\ln[1 - a_{v,2}a_{v,1,a}(1 - e^{-b\cdot LAI_{0,a}})],\end{aligned} \quad (22)$$

by analogy,

$$b\cdot LAI_n = -\ln\left[1 - a_v(n)\left(1 - e^{-b\cdot LAI_{0,a}}\right)\right], \quad (23)$$

where $a_v(n) = a_{v,n}a_{v,n-1,a}\cdots a_{v,1,a}$.

As there is no heterogeneity in zero-order pixel, $a_{v,0}$=1. Compared with the largest heterogeneous patch, if the scale of n order pixel is so large that there are no pure heterogeneity pixel of n–1 order pixel in n order pixel, then m_n=0, so $a_{v,n}$=1.

In other words, if the pixel is big enough, c approaches to a constant determined by the value of $a_v(n)$ of the coarse scale. The relationship between $a_v(n)$ and n can be acquired by numerical simulation (Figure 3).

$$a_v(n) = \frac{1-c}{e^{f(n)}} + c, \quad (24)$$

where c is an undetermined constant determined by the $a_{v,n}$ value of coarse scale. $f(n)$ is a monotonous function increasing progressively with increasing n, and it should satisfy the condition of $f(0)$=0. Normally, it can be assumed as linear increasing function $f(n)$=pn, in which p is an empirical constant.

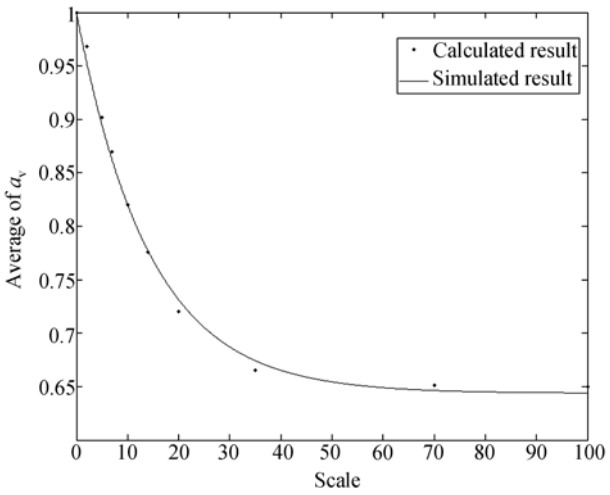

Figure 3 The law of a_v descending with scale.

4.3 Correction for spatial variation of LAI_0

In aforementioned discussion, the assumption neglecting the spatial variation of LAI in the finest pixel (LAI_0) does not accord with reality. It is obvious that the larger the spatial variation of LAI is, the larger the errors caused by it will be. If the variance of LAI_0 ($V_{LAI,0}$) is used to represent the spatial intensity variation of LAI_0, the numerical simulation shows that the retrieving error of LAI ΔLAI_0 is in direct proportion to $V_{LAI,0}$ (Figure 4).

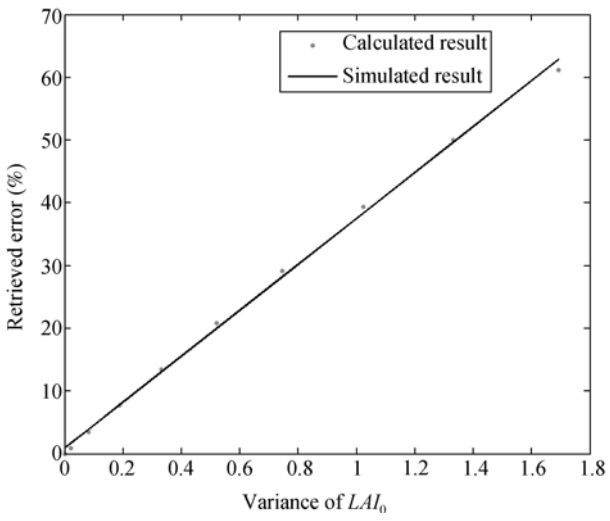

Figure 4 The relationship between the retrieved error of ΔLAI_0 and the variance of LAI_0 ($V_{LAI,0}$).

The correctional formula is

$$LAI_0^* = LAI_{0,a} + m\cdot V_{LAI,0,} \quad (25)$$

where $LAI_{0,a}$ is the retrieved mean true value of *LAI* from formula (23) neglecting the spatial variation of *LAI*, $V_{LAI,0}$ is the variance of $LAI_{0,i}$, and m=0.3589. It is obvious that $V_{LAI,0}$ is unknown, and according to the numerical simulation, the variance of different order scale can be approximated by formula (26):

$$V_{LAI,n} = V_{LAI,0} \cdot \mathrm{e}^{-n}. \tag{26}$$

If the remote sensing image of first-order and second-order scales is known, then

$$V_{LAI,0} = \frac{V_{LAI,1}^2}{V_{LAI,2}}. \tag{27}$$

5 The numerical simulation of *LAI* scaling effect

Make sure the finest spatial scale (supposing it is 1 m), ascertain the random spatial distribution of heterogeneous patch with different scales, and then initialize the $LAI_{0,i}$ of each plant pixel (Figure 5).

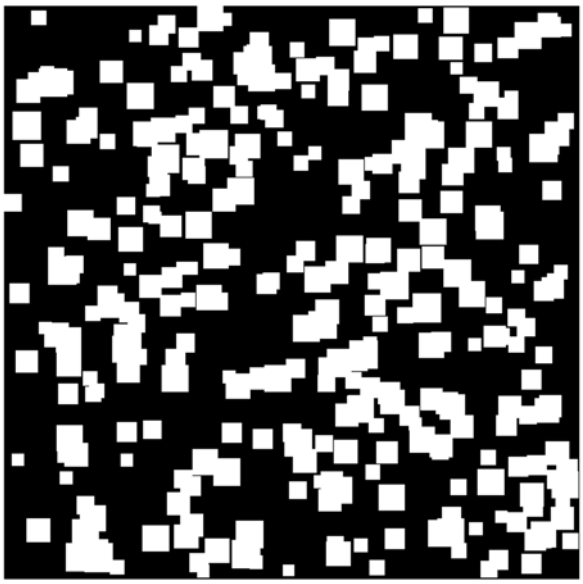

Figure 5 The simulated remote sensing image. White pixels are the pure soil pixels, and the black pixels are pure vegetation pixels.

Suppose the values of ρ_g, ρ_v, G_v, θ_v are known and $\lambda_0 = 1$, in the hotspot direction, as the $LAI_{0,i}$ of every pixel have been ascertained, $\rho_{0,i}$ of each pixel can be calculated according to formula (8), and the spatial distribution of $\rho_{0,i}$ can be obtained. If the relation between the relative pixel scale and order number is $r_R = 3^n$, the zero scale is 1 m × 1 m, the first-order scale is 3 m × 3 m, the second-order scale is 9 m× 9 m and so on and so forth. $\rho_{1,i}$ and $\rho_{2,i}$ distribution image of the first-order, second-order and so on can be created via the summation. Then according to the formula, we have

$$b \cdot LAI_{n,i} = -\ln\left(\frac{\rho_{n,i} - \rho_v}{\rho_g - \rho_v}\right).$$

The retrieval $LAI_{n,i}$ of each order pixel can be derived. Based on the distribution image of $LAI_{0,i}$ and the definition of mixed pixel $LAI_{n,t}$, the distribution image of $LAI_{n,i,t}$ is created. The comparison between retrieved *LAI* and real *LAI* is shown in Table 1. When the real *LAI* is small, the retrieval error is also small. Along with the increase of real *LAI*, the retrieval error also increases, but the relative errors are less than 10%. By the variance correction of $LAI_{n,i}$ using formula (25), the retrieved *LAI* can be acquired. The retrieval errors before and after the variance correction are listed in Table 1.

Table 1 The errors of *LAI* retrieval before and after the variance correction (unit: %)

	Max error	Min error	Average error	SDT
Before correction	6.62	5.90	6.32	6.33
After correction	2.78	0.11	0.81	1.13

6 The scaling transform of remote sensing image

Figure 6 is the SPOT-5 multi-spectrum image of May 6, 2005, of Jining City, Shandong Province, China. The resolution is 10 m. This image consists of 5994×3402 pixels corresponding area of 60 km × 34 km. It is a winter wheat growing season. The ground cover is winter wheat field, villages, water body, roads and so on.

Firstly, radiant calibration and geometric correction are carried out. In order to gain the transfer model of scaled *LAI* from multi-resolution images, we must remove all the other effects, such as atmospheric effect, directional effect caused by bidirectional reflectance of target, and so on, except scaling factor. As a basic material for analysis of spatial scaling effect, the multi-scaling images can only be formed by the same high resolution image through weighted linear summation of radiance of pixels.

Secondly, the classification was applied to images in different scales, and the main categories are vegetation

Figure 6 SPOT-5 multi-spectrum false color composites image of Jining, Shandong Province, China.

(majority of it is winter wheat), town, road, water body and aqueduct and so on. As the spectral characteristic of water body is different from the other categories, the area ratio of water body in coarse resolution image should be indicated. The SPOT-5 image of ten meters can offer the background reflectance of rude pixel in details, so ρ_g is close to the real value. Considering the difference of sun-target-sensor geometry of each pixel, formulae (8) and (10) were used to retrieve *LAI*, meanwhile, formulae (25) and (26) were used to calculate the correction values according to the variance of zero-order *LAI* $V_{LAI,0}$. Results show that the value of LAI_0 is about 3—5, the relative error caused by variance of LAI_0 is about 5%, the heterogeneity is the main reason of scaling effect in this case. Formula (23) can be transformed as follows:

$$e^{-b\cdot LAI_n} = 1-[e^{-pn}(1-c)+c](1-e^{-b\cdot LAI_{0,a}}),$$

where c and $(1-e^{-b\cdot LAI_{0,a}})$ are constant or nearly constant.

$$e^{-b\cdot LAI_n} = (1-D)-B\cdot e^{-pn},$$

$$B = (1-c)(1-e^{-b\cdot LAI_{0,a}}),$$

$$D = c(1-e^{-b\cdot LAI_{0,a}}).$$

So the relationship between LAI_n and number of scale order n is approximately negative linearity. Figure 7 shows the relationship between LAI_n and n in Figure 6, with each curve representing the relationship between LAI_n and n of a 1 km × 1 km pixel, showing that the approximately negative linear relationship between LAI_n and n exists. Since the function of $a_v(n)$ is based on statistical mean and the value of c varies as the size of pixel changes, it is understandable that some of the curves in Figure 7 depart from negative linearity.

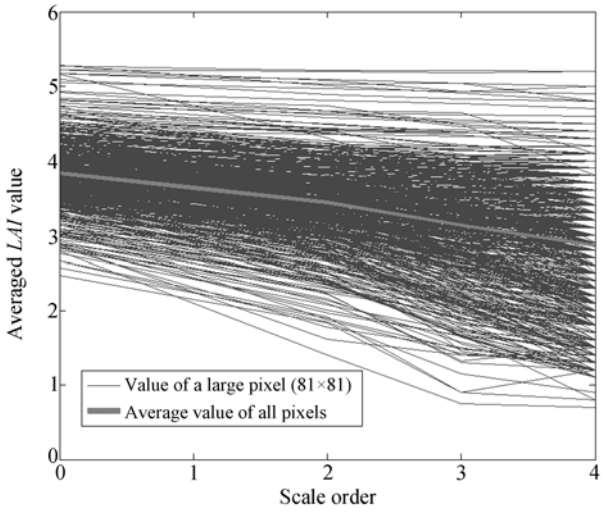

Figure 7 The relationship between *LAI* and scale orders.

7 Conclusions

(1) According to the homogeneous canopy, the spatial scaling effect of retrieved *LAI* exists. The heterogeneity within pixel and non-linearity of retrieving method are the two major reasons.

(2) To the continuous canopy, the formula of scale transform is composed of two parts, the scaling effect caused by heterogeneity can be corrected by formula (23), and the errors caused by spatial variation of $LAI_{0,i}$ can be corrected by formulae (25) and (26).

(3) From the viewpoint of remote sensing, the plant canopy can be classified into two categories, discrete and continuous canopies. As the discreteness is the

characteristic of discrete canopy, the definition of real *LAI* and the retrieval model should be changed, and the scaling effect of discrete canopy should be studied as another independent topic.

1 Badhwar G D, MacDonald R B, Metha N C. Satellite-derived leaf-area-index and vegetation maps as input to global carbon cycle models——A hierarchical approach. Int J Remote Sens, 1986, 7: 265－281
2 Baret F, Guyot G. Potentials and limits of vegetation indices for LAI and APAR assessment. Remote Sens Environ, 1991, 35: 161－173
3 Bicheron P, Leroy M. A method of biophysical parameter retrieval at global scale by inversion of a vegetation reflectance model. Remote Sens Environ, 1999, 67: 251－266
4 Wood E F, Lakshmi V. Scaling water and energy fluxes in climate systems: Three land-atmospheric modeling experiments. J Clim, 1993, 6: 439－857
5 Bonan G B. Land-atmosphere interactions for climate system models: Coupling biophysical, biogeochemical, and ecosystem dynamical processes. Remote Sens Environ, 1995, 51: 57－73
6 Buermann W, Dong J, Zeng X, et al. Evaluation of the utility of satellite-based vegetation leaf area index data for climate simulations. J Clim, 2001, 14(17): 3536－3550
7 Townshend J R G, Justice C O. Selecting the spatial resolution of satellite sensors required for global monitoring of land transformations. Int J Remote Sens, 1988, 9: 187－236
8 Aman A, Randriamanantena H P, Podaire A. Upscale integration of normalized difference vegetation index: The problem of spatial heterogeneity. IEEE Trans Geosci Remote Sensing, 1992, 30: 326－338
9 Bonan G B, Pollard D, Thompson S L. Influence of subgrid-scale heterogeneity in leaf area index, stomatal resistance and soil moisture on grid-scale land-atmosphere interactions. J Clim, 1993, 6: 1882－1897
10 Ehleringer J R, Field C B. Scaling Physiological Processes: Leaf to Globe. Boston: Academic Press, 1993
11 Hall F G, Huemmrich K F, Goetz S J, et al. Satellite remote sensing of surface energy balance: Success, failures, and unresolved issues in FIFE. J Geophys Res, 1992, 97(D17): 19061－19089
12 Hu Z, Islam S. A framework for analyzing and designing scale invariant remote sensing algorithms. IEEE Trans Geosci Remote Sensing, 1997, 35: 747－755
13 Tian Y, Wang Y, Zhang Y, et al. Radiative transfer based scaling of LAI retrievals from reflectance data of different resolutions. Remote Sens Environ, 2003, 84: 143－159
14 Chen J M. Spatial scaling of a remotely sensed surface parameter by contexture. Remote Sens Environ, 1999, 69: 30－42
15 Tian Y H, Woodcock C E, Wang Y J. Multiscale analysis and validation of the MODIS LAI product Ⅰ. Uncertainty assessment. Remote Sens Environ, 2002, 83: 414－430
16 Garrigues S, Allard D, Baret F, et al. Influence of landscape spatial heterogeneity on the non-linear estimation of leaf area index from moderate spatial resolution remote sensing data. Remote Sens Environ, 2006, 105: 286－298
17 Chen J M, Black T A. Defining leaf area index for non-flat leaves. Plant Cell Environ, 1992, 15: 421－429
18 Zhang R, Sun X, Zhu Z. Scale transformation and realistic quantitative remote sensing in IMGRASS (in Chinese). Clim Environ Res, 1997, 2(3): 310－315
19 Li X, Strahler A H. Geometric-optical bidirectional reflectance modeling of a coniferous forest canopy. IEEE Trans Geosci Remote Sensing, 1986, 24: 906－919
20 Chen J M, Leblanc S. A 4-scale bidirectional reflection model based on canopy architecture. IEEE Trans Geosci Remote Sensing, 1997, 35: 1316－1337
21 Nilson T, Kuusk A. A reflectance model for the homogeneous plant canopy and its inversion. Remote Sens Environ, 1989, 27: 157－167
22 Nilson T. Approximate analytical methods for calculating the reflection functions of leaf canopies in remote sensing applications. In: Myneni R B, Ross J, eds. Photon-vegetation Interactions: Applications in Optical Remote Sensing and Plant physiology. Heidelberg-New York: Springer-Verlag, 1991.162－189
23 Xu X. Physics of Remote Sensing (in Chinese). Beijing: Peking University Press, 2005. 47－49
24 Hapke B. Bidirectional reflectance spectroscopy: 1. Theory. J Geophys Res, 1981, 86: 3039－3054
25 Hapke B. Bidirectional reflectance spectroscopy: 4. The extinction coefficient and the opposition effect. Icarus, 1986, 67: 264－280